

# Realized and Planned Improvements in ESA/ESOC Ionosphere Modelling

J. Feltens <sup>1</sup> and J.M. Dow <sup>2</sup>

<sup>1</sup> EDS c/o ESA/ESOC, Robert-Bosch-Straße 5,  
D-64293 Darmstadt, Germany  
Tel: ++49-6151-90-2078  
FAX: ++49-6151-90-3129  
Email: Joachim.Feltens@esa.int

<sup>2</sup> ESA/ESOC, D-64293 Darmstadt, Germany

## Abstract

ESA/ESOC contributes to the activities of the IGS Ionosphere Working Group since the working group's establishment in May 1998. When these activities began, single layer approaches were widely used, and the time resolution of the TEC maps produced was one day. There were also significant gaps in the IGS ground station network at that time. In the meantime especially the time resolution has been enhanced, currently to two hours, and the IGS station coverage could also considerably be densified. The realization of near-real-time processing and real-time processing is under discussion. Beyond these aspects, a clear trend to the establishment of 3-dimensional ionosphere models evaluating "classical" TEC data, derived from GNSS observables, in combination with electron density data obtained from LEO occultations and ground based ionosondes, can be recognized.

At ESA/ESOC the currently still used single layer modelling has been improved with the aid of surface spherical harmonics and to enhance the time resolution, a special estimation scheme has been designed and implemented. Attempts to realize an operational TEC map service locally for the ESA tracking sites will commence soon. Beyond that, activities are ongoing to develop a 3-dimensional ionosphere model which will use "classical" TEC data and electron density data as input. Additionally, there are considerations to establish global and regional ionosphere models based on wavelets.

This paper will provide an overview of the improvements made at ESOC in ionosphere modelling so far, as well as an outlook over further improvements which are currently under development.

## 1 Introduction

Improvements have been made in ESOC ionosphere modelling into several directions. The main achievement is the enhancement of the time resolution for the ESOC Total Electron Content (*TEC*) maps processing and, related with that, changes in the way how TEC maps and Differential Code Biases (*DCBs*) are estimated now.

While the current ionosphere processing at ESOC is still based on a single layer approach, comprehensive developments have been made and are ongoing to realize a 3-dimensional modelling, in which the ionosphere is represented as a composition of several layers.

The upgrades made in the ESOC Ionosphere Monitoring Facility (IONMON) software so far, as well as further improvements which are currently under work will be described in the following chapters.

## 2 IONMON Upgrades so far realized

### 2.1 Enhancement of Time Resolution

In order to enhance the time resolution of the IONMON software, the old batch least squares algorithm has been replaced by a sequential estimate working according to the following principle:

With a certain time resolution, currently set to 2 hours but could also be set to shorter time steps, normal equation systems are established for  $i$  time intervals:

$$\begin{aligned} & \underline{A}_1^T \underline{P}_1 \underline{A}_1 \quad \underline{A}_1^T \underline{P}_1 \underline{l}_1 \quad \underline{l}_1^T \underline{P}_1 \underline{l}_1, \quad \underline{A}_2^T \underline{P}_2 \underline{A}_2 \quad \underline{A}_2^T \underline{P}_2 \underline{l}_2 \quad \underline{l}_2^T \underline{P}_2 \underline{l}_2, \quad \underline{A}_3^T \underline{P}_3 \underline{A}_3 \quad \underline{A}_3^T \underline{P}_3 \underline{l}_3 \quad \underline{l}_3^T \underline{P}_3 \underline{l}_3 \\ & \dots, \quad \underline{A}_{i-1}^T \underline{P}_{i-1} \underline{A}_{i-1} \quad \underline{A}_{i-1}^T \underline{P}_{i-1} \underline{l}_{i-1} \quad \underline{l}_{i-1}^T \underline{P}_{i-1} \underline{l}_{i-1}, \quad \underline{A}_i^T \underline{P}_i \underline{A}_i \quad \underline{A}_i^T \underline{P}_i \underline{l}_i \quad \underline{l}_i^T \underline{P}_i \underline{l}_i \end{aligned} \quad (2.1)$$

where:

$\underline{A}_i$  ... design matrix for the observations of the update  $i$ ,

$\underline{P}_i$  ... observations weight matrix for update  $i$ ,

$\underline{l}_i$  ... vector of observed-minus-computed residuals for update  $i$ .

This archive of normal equation systems is then used in two different ways for *TEC* estimation and for *DCBs* estimation:

#### 1) TEC:

To make an update for the time interval  $i+1$ , the following pseudo-observation equations will be attached to the normal equations  $\underline{A}_{i+1}^T \underline{P}_{i+1} \underline{A}_{i+1} \quad \underline{A}_{i+1}^T \underline{P}_{i+1} \underline{l}_{i+1} \quad \underline{l}_{i+1}^T \underline{P}_{i+1} \underline{l}_{i+1}$ :

$$\begin{bmatrix} 1 & 0 & 0 & \dots & 0 & 0 \\ 0 & 1 & 0 & \dots & 0 & 0 \\ 0 & 0 & 1 & \dots & 0 & 0 \\ \vdots & \vdots & \vdots & \ddots & \vdots & \vdots \\ 0 & 0 & 0 & \dots & 1 & 0 \\ 0 & 0 & 0 & \dots & 0 & 1 \end{bmatrix} \bullet \begin{bmatrix} \Delta \tilde{x}_1 \\ \Delta \tilde{x}_2 \\ \Delta \tilde{x}_3 \\ \vdots \\ \Delta \tilde{x}_{m-1} \\ \Delta \tilde{x}_m \end{bmatrix} = \begin{bmatrix} x_1 - x_{10} \\ x_2 - x_{20} \\ x_3 - x_{30} \\ \vdots \\ x_{(m-1)} - x_{(m-1)0} \\ x_m - x_{m0} \end{bmatrix} \quad (2.2)$$

$$\underline{B} \bullet \underline{\Delta \tilde{x}}_{i+1} = \underline{X}_{i+1}$$

where:

$\underline{B}$  ... design matrix for these pseudo-observations, i.e. a unit matrix,

$\underline{\Delta \tilde{x}}_{i+1}$  ... vector of the corrections to the unknowns for update  $i+1$ ,

$\underline{x}_k$  ... vector of the values of the unknowns in the actual iteration step,

$\underline{x}_{k0}$  ... vector of the values of the unknowns from the previous update  $i$  to which the  $x_k$  shall be constrained to; in the first iteration  $\underline{X}_{i+1}$  is a zero-vector.

Squaring out these pseudo-observation equations into a normal equation system and using a proper weight matrix  $\underline{W}_{i+1}$ , one obtains:

$$\left(\underline{B}^T \underline{W}_{i+1} \underline{B}\right) \bullet \underline{\Delta \tilde{x}}_{i+1} = \underline{B}^T \underline{W}_{i+1} \underline{X}_{i+1} \quad (2.3)$$

Or, since  $\underline{B}$  is a unit matrix:

$$\underline{W}_{i+1} \bullet \underline{\Delta \tilde{x}}_{i+1} = \underline{W}_{i+1} \underline{X}_{i+1} \quad (2.4)$$

The normal equations (2.4) for constraining must then be added to the normal equations  $\underline{A}_{i+1}^T \underline{P}_{i+1} \underline{A}_{i+1} \quad \underline{A}_{i+1}^T \underline{P}_{i+1} \underline{l}_{i+1} \quad \underline{l}_{i+1}^T \underline{P}_{i+1} \underline{l}_{i+1}$  of update  $i+1$ :

$$\begin{aligned} \left(\underline{A}_{i+1}^T \underline{P}_{i+1} \underline{A}_{i+1}\right) \bullet \underline{\Delta \tilde{x}}_{i+1} + \underline{W}_{i+1} \bullet \underline{\Delta \tilde{x}}_{i+1} &= \underline{A}_{i+1}^T \underline{P}_{i+1} \underline{l}_{i+1} + \underline{W}_{i+1} \underline{X}_{i+1} \\ \left(\underline{A}_{i+1}^T \underline{P}_{i+1} \underline{A}_{i+1} + \underline{W}_{i+1}\right) \bullet \underline{\Delta \tilde{x}}_{i+1} &= \underline{A}_{i+1}^T \underline{P}_{i+1} \underline{l}_{i+1} + \underline{W}_{i+1} \underline{X}_{i+1} \end{aligned} \quad (2.5)$$

And the estimated corrections for the unknowns are then:

$$\underline{\Delta \tilde{x}}_{i+1} = \left(\underline{A}_{i+1}^T \underline{P}_{i+1} \underline{A}_{i+1} + \underline{W}_{i+1}\right)^{-1} \bullet \left(\underline{A}_{i+1}^T \underline{P}_{i+1} \underline{l}_{i+1} + \underline{W}_{i+1} \underline{X}_{i+1}\right) \quad (2.6)$$

The weight matrix  $\underline{W}_{i+1}$  in turn is computed from the normal equation systems of the previous updates  $i, i-1, i-2, \dots$  as follows:

$$\underline{W}_{i+1} = \frac{F}{rms_i^2} \bullet \left(f_i \cdot \underline{A}_i^T \underline{P}_i \underline{A}_i + f_{i-1} \cdot \underline{A}_{i-1}^T \underline{P}_{i-1} \underline{A}_{i-1} + f_{i-2} \cdot \underline{A}_{i-2}^T \underline{P}_{i-2} \underline{A}_{i-2} + \dots\right) \quad (2.7)$$

where:

$F$  ... appropriate scaling factor,

$rms_i^2$  ... RMS squared of previous update  $i$ ,

$f_k$  ... scaling factor for the normal matrix of update  $k$ ;  $f_k = e^{-\xi \cdot (t - t_k)}$ ,  $\xi$  ... appropriate scaling factor,  $t$  ... time of current update  $i+1$ ,  $t_k$  ... time of update  $k$  (in this way the influence of older updates is exponentially reduced in the weight matrix).

Once the weight matrix is established with (2.7), the normal equation system (2.6) can be solved to obtain the corrections  $\underline{\Delta \tilde{x}}_{i+1}$  for update  $i+1$  of the unknown ionosphere parameters. The RMS and the mean errors of the unknowns for update  $i+1$  are finally calculated as:

$$\begin{aligned} \underline{\varepsilon}_{i+1}^T \underline{P}_{i+1} \underline{\varepsilon}_{i+1} &= \left(\underline{l}_{i+1}^T \underline{P}_{i+1} \underline{l}_{i+1} + \underline{X}_{i+1}^T \underline{W}_{i+1} \underline{X}_{i+1}\right) - \left(\underline{A}_{i+1}^T \underline{P}_{i+1} \underline{l}_{i+1} + \underline{W}_{i+1} \underline{X}_{i+1}\right)^T \bullet \underline{\Delta \tilde{x}}_{i+1} \\ rms_{i+1} &= \pm \sqrt{\frac{\underline{\varepsilon}_{i+1}^T \underline{P}_{i+1} \underline{\varepsilon}_{i+1}}{n - u}} \end{aligned} \quad (2.8)$$

$$m_x = \pm rms_{i+1} \cdot \sqrt{Q_{xx}} = \pm rms_{i+1} \cdot \sqrt{\left(\underline{A}_{i+1}^T \underline{P}_{i+1} \underline{A}_{i+1} + \underline{W}_{i+1}\right)_x^{-1}}$$

where:

$\underline{\varepsilon}_{i+1}^T \underline{P}_{i+1} \underline{\varepsilon}_{i+1}$  ... squared sum of residuals for update  $i+1$ ,

$rms_{i+1}$  ... *RMS* of update  $i+1$ ;  $n$  ... number of observation equations (incl. the pseudo-observation equations),  $u$  ... number of unknowns (*TEC* parameters & *DCBs*),

$m_x$  ... mean error of an unknown  $x$ .

The normal equations  $\underline{A}_{i+1}^T \underline{P}_{i+1} \underline{A}_{i+1} \quad \underline{A}_{i+1}^T \underline{P}_{i+1} \underline{l}_{i+1} \quad \underline{l}_{i+1}^T \underline{P}_{i+1} \underline{l}_{i+1} \quad rms_{i+1}$  of update  $i+1$  enter then in turn into the establishment of the weight matrix  $\underline{W}_{i+2}$  to constrain update  $i+2$ , and so on ... *TEC* parameters as well as *DCB* values will be estimated during this fit – but only the *TEC* parameters are of interest here.

## 2) *DCBs*:

*DCBs* (for satellites and receivers) fits are done in daily batch estimates. To realize this, the normal equations are put together from the archive (2.1) as follows from all  $d$  normal equations of one day:

$$\left( \underline{A}_1^T \underline{P}_1 \underline{A}_1 + \underline{A}_2^T \underline{P}_2 \underline{A}_2 + \underline{A}_3^T \underline{P}_3 \underline{A}_3 + \dots + \underline{A}_d^T \underline{P}_d \underline{A}_d \right) \bullet \underline{\Delta \tilde{x}} = \underline{A}_1^T \underline{P}_1 \underline{l}_1 + \underline{A}_2^T \underline{P}_2 \underline{l}_2 + \underline{A}_3^T \underline{P}_3 \underline{l}_3 + \dots + \underline{A}_d^T \underline{P}_d \underline{l}_d$$

resp. (2.9)

$$\underline{\Delta \tilde{x}} = \left( \underline{A}_1^T \underline{P}_1 \underline{A}_1 + \underline{A}_2^T \underline{P}_2 \underline{A}_2 + \underline{A}_3^T \underline{P}_3 \underline{A}_3 + \dots + \underline{A}_d^T \underline{P}_d \underline{A}_d \right)^{-1} \bullet \left( \underline{A}_1^T \underline{P}_1 \underline{l}_1 + \underline{A}_2^T \underline{P}_2 \underline{l}_2 + \underline{A}_3^T \underline{P}_3 \underline{l}_3 + \dots + \underline{A}_d^T \underline{P}_d \underline{l}_d \right)$$

The normal equation system (2.9) is then solved to obtain the estimated corrections  $\underline{\Delta \tilde{x}}$  for the unknown *DCB* values for that day. The *RMS* and the mean errors of the unknown *DCBs* are finally calculated as:

$$\underline{\varepsilon}^T \underline{P} \underline{\varepsilon} = \left( \underline{l}_1^T \underline{P}_1 \underline{l}_1 + \underline{l}_2^T \underline{P}_2 \underline{l}_2 + \underline{l}_3^T \underline{P}_3 \underline{l}_3 + \dots + \underline{l}_d^T \underline{P}_d \underline{l}_d \right) - \left( \underline{A}_1^T \underline{P}_1 \underline{l}_1 + \underline{A}_2^T \underline{P}_2 \underline{l}_2 + \underline{A}_3^T \underline{P}_3 \underline{l}_3 + \dots + \underline{A}_d^T \underline{P}_d \underline{l}_d \right)^T \bullet \underline{\Delta \tilde{x}}$$

$$rms = \pm \sqrt{\frac{\underline{\varepsilon}^T \underline{P} \underline{\varepsilon}}{n - u}} \quad (2.10)$$

$$m_D = \pm rms \cdot \sqrt{Q_{DD}} = \pm rms \cdot \sqrt{\left( \underline{A}_1^T \underline{P}_1 \underline{A}_1 + \underline{A}_2^T \underline{P}_2 \underline{A}_2 + \underline{A}_3^T \underline{P}_3 \underline{A}_3 + \dots + \underline{A}_d^T \underline{P}_d \underline{A}_d \right)^{-1}}$$

where:

$\underline{\varepsilon}^T \underline{P} \underline{\varepsilon}$  ... squared sum of residuals,

$rms$  ... *RMS*;  $n$  ... number of observation equations, i.e. the total number of all observations of that day,  $u$  ... number of unknowns (*DCB* values & *TEC* parameters),

$m_D$  ... mean error of an unknown  $D$ .

The solution of the normal equations (2.9) provides the *DCB* values for the satellites and the receivers as well as the *TEC* parameters – but only the *DCB* values are of interest in this fit.

## 2.2 Additional Improvements

Since its upgrade, the IONMON software can produce now, apart from the TEC maps, also RMS maps, which are included into the ESA IONEX files too. The old Gauss Type Exponential Functions approach has been replaced by spherical harmonics as surface functions in order to enhance spatial resolution and to avoid weak modelling around the poles. The Modified Single Layer Model Mapping Function has also been included.

As the weekly combinations of IGS TEC maps show, the ESA TEC maps are now at the same accuracy level as the TEC maps of the other Ionosphere Associate Analysis Centres.

## 3 IONMON Upgrades currently under Work

While the current ESOC ionosphere modelling is still based on a single layer approach, considerable investigations have been made to establish a 3-d ionosphere model. In this model the ionosphere can mathematically be set up as superimposition of several layers (maximal five:  $F_2$ ,  $F_1$ ,  $E$ ,  $D_2$ ,  $D_1$ ), each layer being represented by a separate profile function. Distinct behaviour, e.g. for the influence of the solar zenith angle  $\chi$ , of the different layers can be accounted for. To include the plasmasphere, an exponential correction function with a very large scale height can be added on the topside of the highest layer, namely  $F_2$ . Alternatively, an empirical function for the height dependent scale height can be used, and, as another alternative, bottom – and topside as well as plasmaspheric scale height values can be estimated as constants.

The electron density at a certain altitude is then the sum of the electron densities of the profile functions of all layers at that altitude, plus the plasmaspheric exponential function, and the *TEC* is the sum of the integrals of the profile functions of all layers along the signal path.

Since the observed *TEC* represents the integral over the electron density along signal path, i.e. mathematically the area enclosed by the electron density profile, it is difficult to extract profile shape parameters, like the height  $h_0$  of maximum electron density, from pure *TEC* observables. An estimation of profile shape parameters is only possible with slant range *TEC* data incoming from a lot of different directions, and the spatial resolution remains limited. The estimability of profile shape parameters can be improved by supplementing the *TEC* observables with observed electron densities. The 3-d ionosphere modelling will thus combine GNSS-derived *TEC* data with observed electron density profiles derived from occultations (e.g. Champ, COSMIC or SWARM). The inclusion of digisonde data (Galkin et al., 1999) might be an option too. An additional advantage of occultation data is, that, contrary to *TEC* data which are usually recorded with ground-based GNSS receivers, occultation data are collected at spacecraft, i.e. also over the ocean areas.

The 3-d modelling is conceived for the processing of global *TEC* data in combination with electron density data from globally distributed occultations, i.e. the profile parameters themselves will in turn be expressed in terms of surface functions, e.g. spherical harmonics, depending on geomagnetic latitude and local time, and the coefficients of these surface functions will then be fitted. A proper constraining will be necessary to get a stable separation between the different layers during the estimation process. This requires a fine tuning before the 3-d fits can become operational. – As by-product of the preparatory tests, a small program to perform fits of single profile electron density data is currently established. Before being implemented into the existing IONMON software, the newly established 3-d routines shall be tested with this small program, e.g. to see how good the used profile functions are able to adapt to the observed electron density data, to find out the optimal number of ionosphere layers, i.e. number of combined profiles, to be used, to tune the *TEC* integrator, etc. After these tests, this small program could also be used operationally for single profile analysis.

### 3.1 Profile Functions

More information about the 3-d ionosphere modelling can be found in Feltens (2002), and after the software upgrade has been concluded, a technical note containing the detailed mathematical model description will be established. As part of the mathematical modelling, also several profile functions were worked out (Feltens, 2002), of which two shall be presented in this paper as example. The first one is the **MacLaurin Series Expansion of the Chapman Profile Function**: The development of the Chapman Profile Function into a MacLaurin Series Expansion offers the possibility to fit observed electron density profile data to such a series expansion, i.e. estimating corrections to the series expansion coefficients - and the estimated offsets with respect to the initial coefficients of the series expansion can be interpreted as deviation of the observed profile from an ideal Chapman Profile. As will also be shown below, the series expansion offers an alternative method to compute the profile integral value, which is essential for TEC observations processing. However, as will be seen from the subsequent formulae too, the series expansion will require increased computer processing load.

The mathematical developments for the MacLaurin Series Expansion commence with the  $\alpha$ -layer Chapman Profile Function (only the basic principle can be shown here):

$$e^{\alpha(1-\sec\chi\cdot e^{-z})} \underset{\text{def.}}{=} e^{\alpha(1-z)} \cdot e^{-\alpha\cdot\sec\chi\cdot e^{-z}} \underset{\text{def.}}{=} e^{\alpha(1-z)} \cdot e^{-\gamma\cdot e^{-z}} \quad ; \quad \gamma \underset{\text{def.}}{=} \alpha \cdot \sec\chi \quad (3.1)$$

with  $z = (h - h_0)/H$ ;  $h$  ... height above ground,  $h_0$  ... height of maximum electron density,  $H$  ... scale height.

Concerning *TEC* integration,  $\sec\chi$  and thus  $\gamma$  is assumed to be constant in equation (3.1), i.e. not varying with altitude. – The variation of the solar zenith angle  $\chi$  is accounted for the summation formula of the *TEC* integrator, which cannot be further detailed in this paper.

The term  $e^{-\gamma\cdot e^{-z}}$  can now be expanded into a MacLaurin Series Expansion:

$$f(z) = f(0) + \frac{f'(0)}{1!} \cdot z + \frac{f''(0)}{2!} \cdot z^2 + \frac{f'''(0)}{3!} \cdot z^3 + \dots$$

Building the derivatives of  $e^{-\gamma\cdot e^{-z}}$  up to ten:

$$\begin{aligned} f(z) &= e^{-\gamma\cdot e^{-z}} \\ f'(z) &= (\gamma \cdot e^{-z}) \cdot e^{-\gamma\cdot e^{-z}} \\ f''(z) &= -1 \cdot (\gamma \cdot e^{-z} - \gamma^2 \cdot e^{-2z}) \cdot e^{-\gamma\cdot e^{-z}} \\ f'''(z) &= (\gamma \cdot e^{-z} - 3\gamma^2 \cdot e^{-2z} + \gamma^3 \cdot e^{-3z}) \cdot e^{-\gamma\cdot e^{-z}} \\ f^{(4)}(z) &= -1 \cdot (\gamma \cdot e^{-z} - 7\gamma^2 \cdot e^{-2z} + 6\gamma^3 \cdot e^{-3z} - \gamma^4 \cdot e^{-4z}) \cdot e^{-\gamma\cdot e^{-z}} \\ f^{(5)}(z) &= (\gamma \cdot e^{-z} - 15\gamma^2 \cdot e^{-2z} + 25\gamma^3 \cdot e^{-3z} - 10\gamma^4 \cdot e^{-4z} + \gamma^5 \cdot e^{-5z}) \cdot e^{-\gamma\cdot e^{-z}} \\ f^{(6)}(z) &= -1 \cdot (\gamma \cdot e^{-z} - 31\gamma^2 \cdot e^{-2z} + 90\gamma^3 \cdot e^{-3z} - 65\gamma^4 \cdot e^{-4z} + 15\gamma^5 \cdot e^{-5z} - \gamma^6 \cdot e^{-6z}) \cdot e^{-\gamma\cdot e^{-z}} \\ f^{(7)}(z) &= (\gamma \cdot e^{-z} - 63\gamma^2 \cdot e^{-2z} + 301\gamma^3 \cdot e^{-3z} - 350\gamma^4 \cdot e^{-4z} + 140\gamma^5 \cdot e^{-5z} - 21\gamma^6 \cdot e^{-6z} + \gamma^7 \cdot e^{-7z}) \cdot e^{-\gamma\cdot e^{-z}} \\ f^{(8)}(z) &= -1 \cdot (\gamma \cdot e^{-z} - 127\gamma^2 \cdot e^{-2z} + 966\gamma^3 \cdot e^{-3z} - 1701\gamma^4 \cdot e^{-4z} + 1050\gamma^5 \cdot e^{-5z} - 266\gamma^6 \cdot e^{-6z} + 28\gamma^7 \cdot e^{-7z} - \gamma^8 \cdot e^{-8z}) \cdot e^{-\gamma\cdot e^{-z}} \\ f^{(9)}(z) &= (\gamma \cdot e^{-z} - 255\gamma^2 \cdot e^{-2z} + 3025\gamma^3 \cdot e^{-3z} - 7770\gamma^4 \cdot e^{-4z} + 6951\gamma^5 \cdot e^{-5z} - 2646\gamma^6 \cdot e^{-6z} + 462\gamma^7 \cdot e^{-7z} - 36\gamma^8 \cdot e^{-8z} + \gamma^9 \cdot e^{-9z}) \cdot e^{-\gamma\cdot e^{-z}} \\ f^{(10)}(z) &= -1 \cdot (\gamma \cdot e^{-z} - 511\gamma^2 \cdot e^{-2z} + 9330\gamma^3 \cdot e^{-3z} - 34105\gamma^4 \cdot e^{-4z} + 42525\gamma^5 \cdot e^{-5z} - 22827\gamma^6 \cdot e^{-6z} + 5880\gamma^7 \cdot e^{-7z} - 750\gamma^8 \cdot e^{-8z} + 45\gamma^9 \cdot e^{-9z} - \gamma^{10} \cdot e^{-10z}) \cdot e^{-\gamma\cdot e^{-z}} \\ &\vdots \end{aligned}$$

Evaluating the derivatives at  $z = 0$ :

$$\begin{aligned}
f(0) &= e^{-\gamma} \\
f'(0) &= (\gamma) \cdot e^{-\gamma} \\
f''(0) &= -1 \cdot (\gamma - \gamma^2) \cdot e^{-\gamma} \\
f'''(0) &= (\gamma - 3\gamma^2 + \gamma^3) \cdot e^{-\gamma} \\
f^{(4)}(0) &= -1 \cdot (\gamma - 7\gamma^2 + 6\gamma^3 - \gamma^4) \cdot e^{-\gamma} \\
f^{(5)}(0) &= (\gamma - 15\gamma^2 + 25\gamma^3 - 10\gamma^4 + \gamma^5) \cdot e^{-\gamma} \\
f^{(6)}(0) &= -1 \cdot (\gamma - 31\gamma^2 + 90\gamma^3 - 65\gamma^4 + 15\gamma^5 - \gamma^6) \cdot e^{-\gamma} \\
f^{(7)}(0) &= (\gamma - 63\gamma^2 + 301\gamma^3 - 350\gamma^4 + 140\gamma^5 - 21\gamma^6 + \gamma^7) \cdot e^{-\gamma} \\
f^{(8)}(0) &= -1 \cdot (\gamma - 127\gamma^2 + 966\gamma^3 - 1701\gamma^4 + 1050\gamma^5 - 266\gamma^6 + 28\gamma^7 - \gamma^8) \cdot e^{-\gamma} \\
f^{(9)}(0) &= (\gamma - 255\gamma^2 + 3025\gamma^3 - 7770\gamma^4 + 6951\gamma^5 - 2646\gamma^6 + 462\gamma^7 - 36\gamma^8 + \gamma^9) \cdot e^{-\gamma} \\
f^{(10)}(0) &= -1 \cdot (\gamma - 511\gamma^2 + 9330\gamma^3 - 34105\gamma^4 + 42525\gamma^5 - 22827\gamma^6 + 5880\gamma^7 - 750\gamma^8 + 45\gamma^9 - \gamma^{10}) \cdot e^{-\gamma} \\
&\vdots
\end{aligned}$$

Defining  $\gamma$ -dependent coefficients:

$$\begin{aligned}
c_1 &= (\gamma) \\
c_2 &= -1 \cdot (\gamma - \gamma^2) \\
c_3 &= (\gamma - 3\gamma^2 + \gamma^3) \\
c_4 &= -1 \cdot (\gamma - 7\gamma^2 + 6\gamma^3 - \gamma^4) \\
c_5 &= (\gamma - 15\gamma^2 + 25\gamma^3 - 10\gamma^4 + \gamma^5) \\
c_6 &= -1 \cdot (\gamma - 31\gamma^2 + 90\gamma^3 - 65\gamma^4 + 15\gamma^5 - \gamma^6) \\
c_7 &= (\gamma - 63\gamma^2 + 301\gamma^3 - 350\gamma^4 + 140\gamma^5 - 21\gamma^6 + \gamma^7) \\
c_8 &= -1 \cdot (\gamma - 127\gamma^2 + 966\gamma^3 - 1701\gamma^4 + 1050\gamma^5 - 266\gamma^6 + 28\gamma^7 - \gamma^8) \\
c_9 &= (\gamma - 255\gamma^2 + 3025\gamma^3 - 7770\gamma^4 + 6951\gamma^5 - 2646\gamma^6 + 462\gamma^7 - 36\gamma^8 + \gamma^9) \\
c_{10} &= -1 \cdot (\gamma - 511\gamma^2 + 9330\gamma^3 - 34105\gamma^4 + 42525\gamma^5 - 22827\gamma^6 + 5880\gamma^7 - 750\gamma^8 + 45\gamma^9 - \gamma^{10}) \\
&\vdots
\end{aligned} \tag{3.2}$$

One finally obtains the MacLaurin Series Expansion for  $e^{-\gamma \cdot e^{-z}}$ :

$$e^{-\gamma \cdot e^{-z}} \approx R(z) = \frac{1}{e^\gamma} \cdot \left\{ 1 + c_1 \cdot z + \frac{c_2}{2!} \cdot z^2 + \frac{c_3}{3!} \cdot z^3 + \dots \right\} \tag{3.3}$$

Replacing  $e^{-\gamma \cdot e^{-z}}$  in (3.1) now by its series expansion (3.3), one gets the following profile function:

$$e^{\alpha(1-z)} \cdot e^{-\gamma \cdot e^{-z}} \approx e^{\alpha(1-z)} \cdot R(z) = e^{\alpha(1-z)} \cdot \frac{1}{e^\gamma} \cdot \left\{ 1 + c_1 \cdot z + \frac{c_2}{2!} \cdot z^2 + \frac{c_3}{3!} \cdot z^3 + \dots \right\}$$

With  $e^{\alpha(1-z)} \cdot e^{-\gamma} = e^{\alpha(1-\sec \chi)} \cdot e^{-\alpha z}$  follows:

$$e^{\alpha(1-z)} \cdot e^{-\gamma \cdot e^{-z}} \approx e^{\alpha(1-z)} \cdot R(z) = e^{\alpha(1-\sec \chi)} \cdot e^{-\alpha z} \cdot \left\{ 1 + c_1 \cdot z + \frac{c_2}{2!} \cdot z^2 + \frac{c_3}{3!} \cdot z^3 + \dots \right\} \quad (3.4)$$

And for the *TEC* integral:

$$\begin{aligned} \int \left( e^{\alpha(1-z)} \cdot e^{-\gamma \cdot e^{-z}} \right) dz &\approx \int \left( e^{\alpha(1-z)} \cdot R(z) \right) dz = e^{\alpha(1-\sec \chi)} \cdot \int e^{-\alpha z} \cdot \left\{ 1 + c_1 \cdot z + \frac{c_2}{2!} \cdot z^2 + \frac{c_3}{3!} \cdot z^3 + \dots \right\} dz \\ &= e^{\alpha(1-\sec \chi)} \cdot \left\{ \int e^{-\alpha z} dz + c_1 \cdot \int z \cdot e^{-\alpha z} dz + \frac{c_2}{2!} \cdot \int z^2 \cdot e^{-\alpha z} dz + \frac{c_3}{3!} \cdot \int z^3 \cdot e^{-\alpha z} dz + \dots \right\} \end{aligned} \quad (3.5)$$

The integral terms in equation (3.5) can be solved recursively, starting with  $\int e^{-\alpha z} dz = -\frac{1}{\alpha} \cdot e^{-\alpha z}$  :

$$\begin{aligned} \int z \cdot e^{-\alpha z} dz &= -\frac{1}{\alpha} \cdot z \cdot e^{-\alpha z} + \frac{1}{\alpha} \cdot \int e^{-\alpha z} dz \\ \int z^2 \cdot e^{-\alpha z} dz &= -\frac{1}{\alpha} \cdot z^2 \cdot e^{-\alpha z} + \frac{2}{\alpha} \cdot \int z \cdot e^{-\alpha z} dz \\ \int z^3 \cdot e^{-\alpha z} dz &= -\frac{1}{\alpha} \cdot z^3 \cdot e^{-\alpha z} + \frac{3}{\alpha} \cdot \int z^2 \cdot e^{-\alpha z} dz \\ \int z^4 \cdot e^{-\alpha z} dz &= -\frac{1}{\alpha} \cdot z^4 \cdot e^{-\alpha z} + \frac{4}{\alpha} \cdot \int z^3 \cdot e^{-\alpha z} dz \\ \int z^5 \cdot e^{-\alpha z} dz &= -\frac{1}{\alpha} \cdot z^5 \cdot e^{-\alpha z} + \frac{5}{\alpha} \cdot \int z^4 \cdot e^{-\alpha z} dz \\ &\vdots \\ \int z^n \cdot e^{-\alpha z} dz &= -\frac{1}{\alpha} \cdot z^n \cdot e^{-\alpha z} + \frac{n}{\alpha} \cdot \int z^{(n-1)} \cdot e^{-\alpha z} dz = \frac{1}{\alpha} \cdot \left\{ -z^n \cdot e^{-\alpha z} + n \cdot \int z^{(n-1)} \cdot e^{-\alpha z} dz \right\} \end{aligned} \quad (3.6)$$

The scheme (3.6) can also be applied purely numerically for a given  $z$ -value, i.e. starting with the knowledge of the numerical value for  $\int e^{-\alpha z} dz = -\frac{1}{\alpha} \cdot e^{-\alpha z}$ , it is easy to calculate the numerical value of  $\int z \cdot e^{-\alpha z} dz$ . This number can then in turn be used to get the value for  $\int z^2 \cdot e^{-\alpha z} dz$ , ... and so on. This means that all these integrals can be evaluated purely numerically in a loop up to the desired series expansion degree  $n$  – without explicit knowledge of their individual analytical formulae.

Finally a recursion formula must be set up for the computation of the  $\gamma$ -dependent coefficients  $c_i$ . When inspecting equations (3.2) one recognizes that the  $c_i$  are principally sums of terms  $a_{ik} \cdot \gamma^k$ , where  $\gamma = \alpha \cdot \sec \chi$ , i.e.  $\gamma$  is varying and the  $a_{ik}$  are non-varying constants. For these constant coefficients  $a_{ik}$  a recursion formula can be set up too. To establish the recursion algorithm, the coefficients  $a_{ik}$  for the  $c_i$  of the different derivatives  $f^{(i)}(z)$  are extracted from equations (3.2) and put together in triangular form as follows (where  $i$  stands for the  $i^{th}$  derivative and the index  $k$  runs over all  $k = 1, \dots, i$  non-varying constants  $a_{ik}$  for that derivative):



$$\begin{array}{c|cccccc}
f'(z) & a_{11} & & & & & \\
f''(z) & a_{21} & a_{22} & & & & \\
f'''(z) & a_{31} & a_{32} & a_{33} & & & \\
f^{(4)}(z) & a_{41} & a_{42} & a_{43} & a_{44} & & \\
f^{(5)}(z) & \vdots & & & & \ddots & 
\end{array}$$

Taking the numbers from equations (3.2), one gets thus the following triangle for the first ten derivatives:

$$\begin{array}{c|cccccccccc}
f'(z) & 1 & & & & & & & & & \\
f''(z) & -1 & 1 & & & & & & & & \\
f'''(z) & 1 & -3 & 1 & & & & & & & \\
f^{(4)}(z) & -1 & 7 & -6 & 1 & & & & & & \\
f^{(5)}(z) & 1 & -15 & 25 & -10 & 1 & & & & & \\
f^{(6)}(z) & -1 & 31 & -90 & 65 & -15 & 1 & & & & \\
f^{(7)}(z) & 1 & -63 & 301 & -350 & 140 & -21 & 1 & & & \\
f^{(8)}(z) & -1 & 127 & -966 & 1701 & -1050 & 266 & -28 & 1 & & \\
f^{(9)}(z) & 1 & -255 & 3025 & -7770 & 6951 & -2646 & 462 & -36 & 1 & \\
f^{(10)}(z) & -1 & 511 & -9330 & 34105 & -42525 & 22827 & -5880 & 750 & -45 & 1
\end{array}$$

From the above triangle the following recursion formula can be derived for the coefficients  $a_{ik}$  :

$$a_{11} = +1$$

$$a_{21} = -1, \quad a_{22} = +1$$

$$a_{i1} = (-1)^{i-1}, \quad \text{for } k = 1$$

$$a_{ik} = (-1)^{i-k} \cdot \left\{ |a_{i-1,k}| \cdot k + |a_{i-1,k-1}| \right\}, \quad \text{for } k = 2, \dots, i-1 \quad (3.7)$$

$$a_{ii} = +1, \quad \text{for } k = i$$

where

$$i \dots i^{th} \text{ derivative}, \quad k = 1, \dots, i$$

In this way an  $\alpha$ -layer Chapman Profile can be replaced by a MacLaurin Series Expansion, which can be evaluated by a combination of recursion formulae, and the integral as well.

### Analyt. Profile Function vs Series Expansion, $\alpha = 1/2$

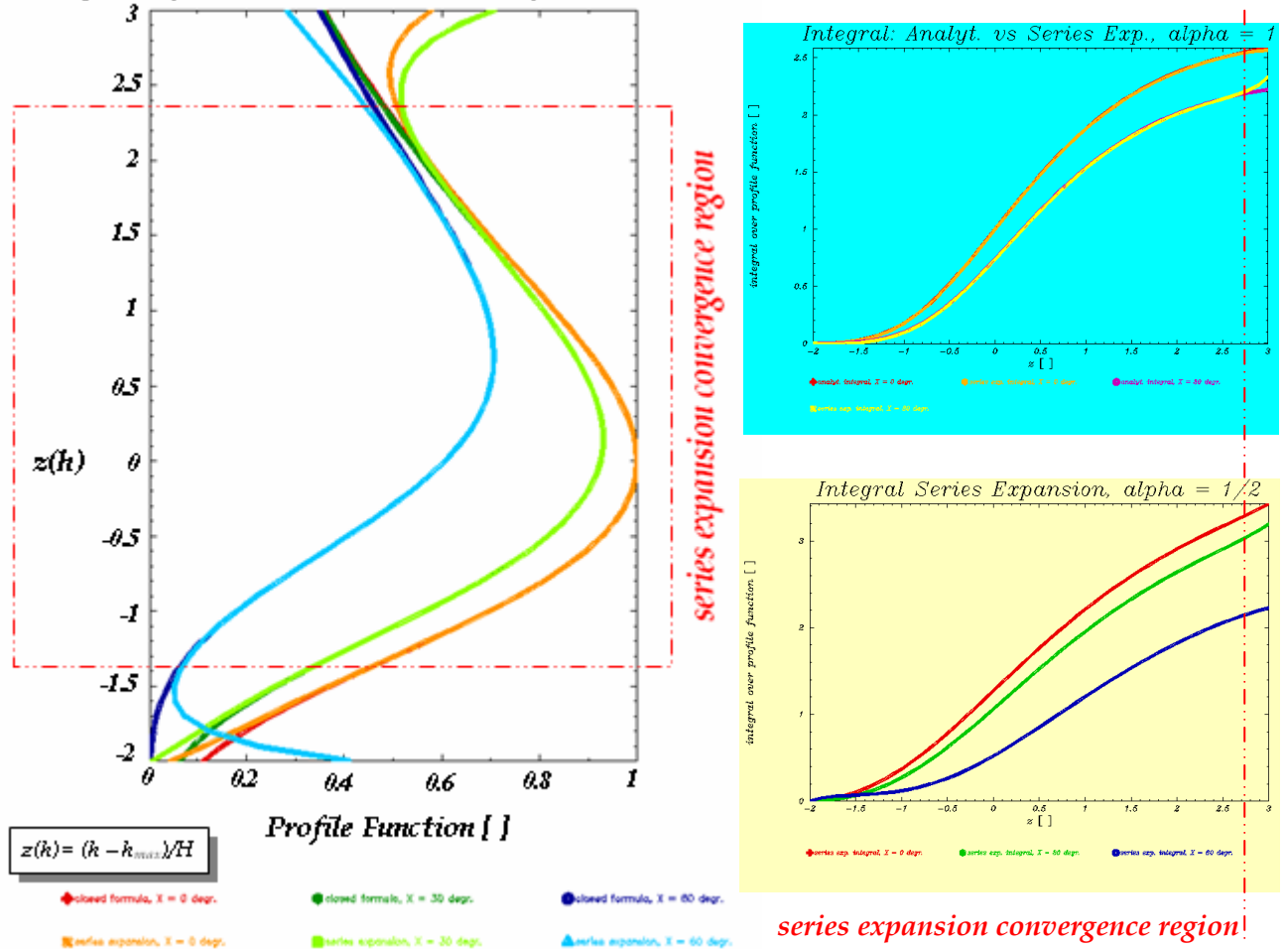


**Figure 3-1:** Chapman Profile Function vs MacLaurin Series Expansion.

The left part of Figure 3-1 shows the curve of the Chapman Profile formula versus the series expansion of degree 10 for the solar zenith angles  $\chi = 0^\circ$  (red),  $30^\circ$  (green),  $60^\circ$  (blue) (the dark colours are the curves of the closed formula, the pale colours are the curves of the series expansion). The blue top right part of the figure displays the curves of the analytical integral of the Chapman Profile Function versus the integral of the series expansion for  $\alpha = 1$  and  $\chi = 0^\circ$  (orange vs red),  $30^\circ$  (yellow vs violet), and the yellow bottom right part the curves for the series expansion integral, for  $\alpha = 1/2$  and  $\chi = 0^\circ$  (red),  $30^\circ$  (green),  $60^\circ$  (blue). It can be seen that the convergence region of the series expansion extends from  $z \approx -1.5 \leftrightarrow z \approx +2.5$ , depending on solar zenith angle  $\chi$ , i.e. the central part of the profile is covered by the series expansion. For the modelling of the parts outside the convergence region, the series expansion is replaced by auxiliary exponential functions – it is beyond the scope of this paper to go into further detail about that. Concerning the evaluation of the integral from the series expansion, the integral values obtained are biased with respect to the ones obtained from the analytical formulae (for  $\alpha = 1$ ) by big integration constants, but when differencing between successive integral values, these constants cancel and the integral curves in Figure 3-1 were obtained by subtracting from all series expansion integral values the corresponding integral value of the lowest possible  $z$  within the

convergence region (where the values of the analytical integral converge to zero). The amount of the integration constant depends on degree  $n$  of series expansion development, solar zenith angle  $\gamma$  and  $\alpha$ -value.

From fits of observed electron density profiles to this series expansion profile function, corrections  $\delta c_i$  to the  $\gamma$ -dependent coefficients  $c_i$  can be obtained, where the offsets  $\delta c_i$  describe the deviation of the observed profile from an idealized Chapman Profile:

$$\tilde{c}_i(\gamma) = c_i(\gamma) + \gamma^x \cdot \delta c_i \quad (3.8)$$

where

$x$  ... fixed constant.

A second profile function, which has been developed for the 3-d ionosphere modelling, can only be shortly mentioned at the end of this Section 3.1: The **superimposition of the Chapman Profile Function with its mirrored counterpart**. The Chapman Profile has a fixed ratio of topside electron density with respect to bottomside electron density. One way to change this ratio is to combine the Chapman Profile with its mirrored counterpart. The formula development starts with the analytical integral function of the Chapman Profile (for  $\alpha = 1$ ):

$$\text{Chapman Profile: } ICP(x) = e^{(1-e^{-x})} \quad \Rightarrow \quad \text{mirrored function: } ICP_{mirr}(x) = e^{(1-e^{+x})}$$

Combine both integral functions as follows:

$$\begin{aligned} P(x) &= (1-L) \cdot ICP(x) - L \cdot ICP_{mirr}(x) \\ &= (1-L) \cdot e^{(1-e^{-x})} - L \cdot e^{(1-e^{+x})} = e^{(1-e^{-x})} + L \cdot \left\{ -e^{(1-e^{-x})} - e^{(1-e^{+x})} \right\} \quad \text{for } 0 \leq L \leq 1 \end{aligned} \quad (3.9)$$

where

$P(x)$  ... profile function integral of the combined curve,

$L$  ... combination factor  $0 \leq L \leq 1$  telling at which %-ual ratio the Chapman Profile and its mirrored counterpart shall be combined.

The first derivative of this profile function integral with respect to  $x$  is then the profile function itself:

$$p(x) = e^{(1-x-e^{-x})} + L \cdot \left\{ -e^{(1-x-e^{-x})} + e^{(1+x-e^{+x})} \right\} \quad (3.10)$$

Figure 3-2 shows the profile functions resulting from combination of the Chapman Profile with its mirrored counterpart for  $L = 0.0, 0.3, 0.5, 0.7, 1.0$ .  $L = 0.0$  (dark blue curve) corresponds to a pure Chapman Profile,  $L = 0.5$  (orange curve) corresponds to the mean of the Chapman Profile and its mirrored counterpart and is a symmetric profile with respect to the height  $h_0$  of maximum electron density, and  $L = 1.0$  (dark red curve) would correspond to the pure mirrored Chapman Profile. – For the real ionosphere only  $L$ -values in the range of  $0 \leq L < 0.5$  might be of relevance.

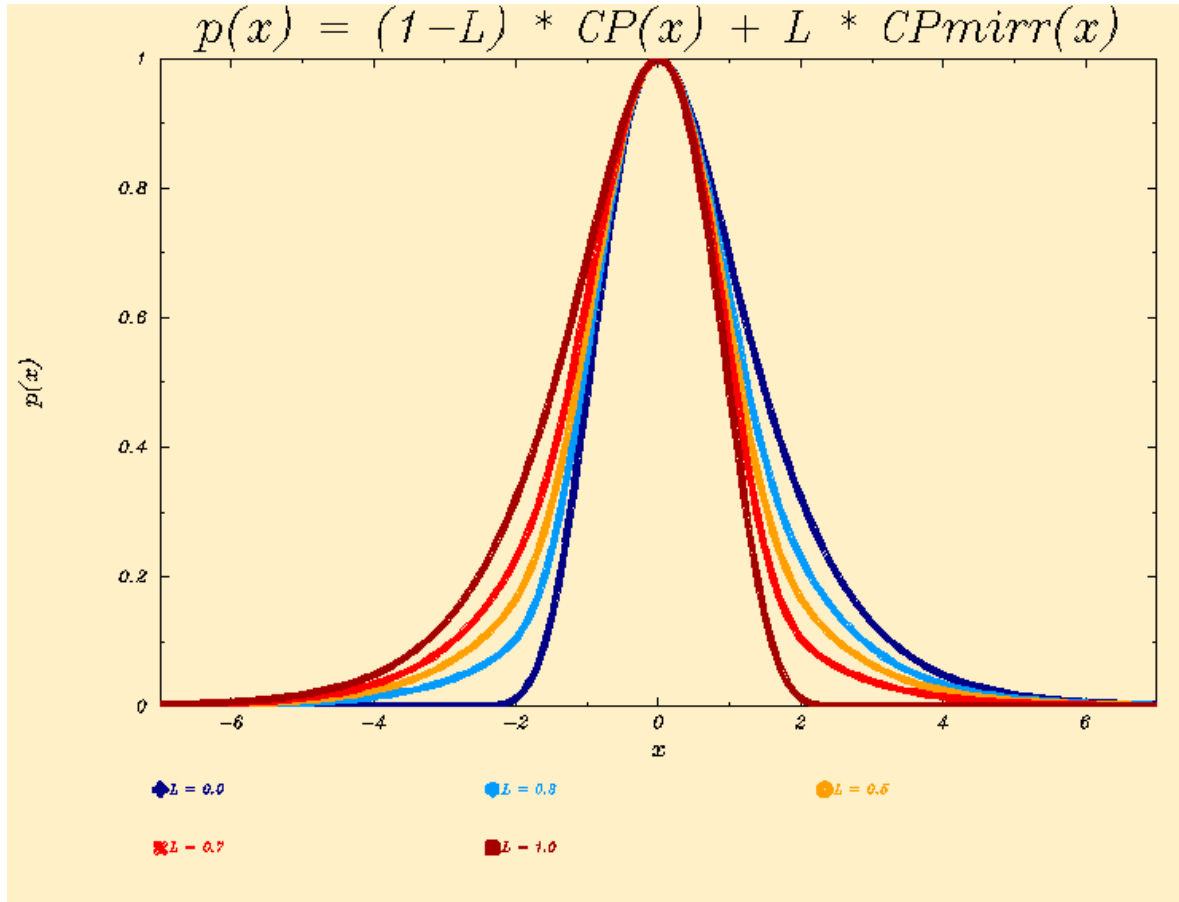


**Figure 3-2:** Profile functions obtained by combining the Chapman Profile Function with its mirrored counterpart for  $0 \leq L \leq 1$ .

Expressed in the general form with the solar zenith distance  $\chi$  included, the functions of the profile and the integral are (Feltens, 2002):

$$p(z, \chi) = e^{(1-z-\sec \chi \cdot e^{-z})} + L \cdot \left\{ -e^{(1-z-\sec \chi \cdot e^{-z})} + \cos^2 \chi \cdot e^{(1+z-\cos \chi \cdot e^{+z})} \right\} \quad (3.11a)$$

$$P(z, \chi) = \cos \chi \cdot e^{(1-\sec \chi \cdot e^{-z})} + L \cdot \left\{ -\cos \chi \cdot e^{(1-\sec \chi \cdot e^{-z})} - \cos \chi \cdot e^{(1-\cos \chi \cdot e^{+z})} \right\} \quad (3.11b)$$

Factor  $L$  can be determined from a profile fit to observed electron density data. The observed profile can then be interpreted as being composed by  $(1-L)$  % of a Chapman Profile and by  $L$  % of the Chapman Profile's mirrored counterpart.

### 3.2 Current Implementation Status

The mathematical algorithms for 3-d ionosphere modelling have been worked out, coded and unit tested. Prior to the implementation of the new routines into the IONMON software, additional tests and validations will be performed, e.g. to find an optimal combination of profile functions for the different ionosphere layers, to find a proper combination of parameters to be estimated, to find an optimal step width for the TEC integrator, etc. Currently (May 2006), as part of these tests, a small program to perform fits to single electron density profiles, invoking the new 3-d model routines, is under preparation. From its conception, this small program could later on also be used operationally

for single profile analyses. After the tests are concluded, the new 3-d model routines will be implemented into the IONMON software and final tests will be made. Thereafter the new 3-d ionosphere model will be ready for operational use and the complete mathematical algorithms will be electronically documented.

#### **4 Future Upgrades**

The inclusion of TEC observables derived from other GNSS data than GPS, namely GLONASS and Galileo, into the IONMON processing is under preparation. Also the inclusion of further sources of observed electron density data will be considered.

The IONMON External User Interface, which allows to access the ionosphere models directly via their estimated coefficients and not indirectly via IONEX files, has to be adapted to the new modelling. Also the currently existing very simple tool to predict the ionosphere's state has significantly to be upgraded.

The possibility to establish wavelet-based ionosphere modelling is considered, see e.g. (Mautz et al., 2005), and also the aspect of the so called "higher order terms".

#### **5 Conclusions**

The ESOC ionosphere modelling has been improved into several directions: The time resolution as well as the spatial resolution of the ESA ionosphere models were enhanced, resulting in a considerable increase of accuracy. Beyond that, smaller upgrades, e.g. the implementation of the Modified Single Layer Model Mapping Function, the inclusion of data from more ground sites, and others, were done. The processing of TEC data originating from GLONASS and Galileo is under preparation. The routine establishment of local ionosphere models for the ESA tracking sites shall commence soon.

Significant progress has been made in the development of a 3-dimensional ESOC ionosphere model. This model takes into account that the ionosphere is composed of several layers. Beyond "classical" TEC data, also electron density observation data originating from different sources will be included into the 3-d processing. Exemplarily for the mathematical algorithms developed for 3-d modelling, the basics of two newly developed profile functions have been presented in this paper.

Further developments and upgrades are planned.

#### **References**

- Feltens, J., 2002, Current Status of ESOC Ionosphere Modeling and Planned Improvements, IGS Presentation, in Collection of Papers and Viewgraphs of the IGS/IAACs Ionosphere Workshop, ESOC, Darmstadt, Germany, January 17-18, 2002 (a PDF version of this paper can be obtained upon request from [Joachim.Feltens@esa.int](mailto:Joachim.Feltens@esa.int)).
- Galkin, I.A., B.W. Reinisch and D.F. Kitrosser, 1999, Advances in Digisonde Networking, in Proceedings of the 1999 International Ionospheric Effects Symposium (IES99), Ramada Hotel Old Town, Alexandria, Virginia, U.S.A., May 4-6, 1999, pp 166-171.
- Mautz, R., J. Ping, K. Heki, B. Schaffrin, C. Shum and L. Potts, 2005, Efficient spatial and temporal representations of global ionosphere maps over Japan using B-spline wavelets, *Journal of Geodesy* 78: 660-667, 2005.